

Exact quark mass corrections to Higgs production in association with a jet

Gábor Somogyi
HUN-REN Wigner Research Centre for Physics



with R. Bonciani, V. Del Duca, H. Frellesvig, M. Hidding, V. Hirschi, F. Moriello, G. Salvatori, GS and F. Tramontano, Phys. Lett. B **843** (2023), 137995, [[arXiv:2206.10490](https://arxiv.org/abs/2206.10490)] [[hep-ph](#)]



The role of precision

The **discovery of the Higgs boson** by the ATLAS and CMS collaborations at the CERN LHC in 2012 is a milestone of particle physics: a **spectacular confirmation of the Standard Model** of elementary particles.

However, great questions remain

- What is dark matter and dark energy?
- How does baryogenesis happen?
- Why are neutrinos so light?
- What is the origin of flavor and CP violation?
- Is our vacuum stable on cosmological timescales?
- ...

In short, what comes beyond the Standard Model?

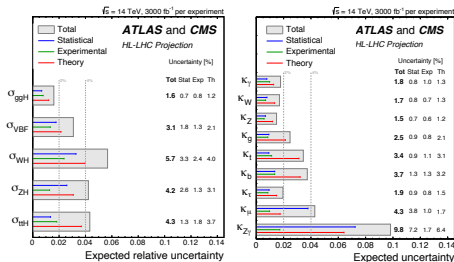
The detection of direct signals of BSM physics has thus far eluded us at the LHC. Thus, focusing on possible small deviations between measurements and SM predictions is of paramount importance.

First signs of New Physics may well be indirect: precision is key!

The role of precision

The High Luminosity LHC program (3 ab⁻¹ integrated luminosity per experiment) is expected to measure Higgs boson production cross sections and couplings to an accuracy of $\sim 2\text{--}4\%$.

- This is precise enough to constrain the parameter spaces of many BSM models.
- The forecasts in the presented figures **assume a substantial decrease of current theoretical uncertainties.**
- The role of theoretical uncertainties is especially noteworthy for the couplings to t - and b -quarks and gluons.



[ATLAS coll., ATL-PHYS-PUB-2022-018]

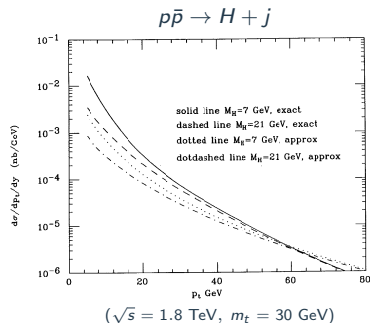
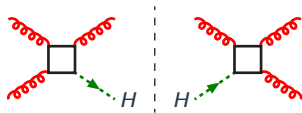
Formidable task to search for deviations by comparing accurate measurements and precise theoretical predictions: **this is precision work!**

Why Higgs + jet production

The dominant Higgs production mode at the LHC is gluon fusion with the coupling of the Higgs boson to gluons mediated by a heavy quark loop.

- The study of Higgs + jet production provides important information about the coupling of the Higgs boson to the virtual particles circulating in the loop.
- The boosted regime allows for a clean signature for the Higgs decay products.
- The exact LO calculation with an arbitrary internal fermion mass was performed more than 30 years ago!

[Ellis, Hinchliffe, Soldate and Van der Bij 1988]



Higgs + jet production at the LHC: state-of-the art

We study Higgs + jet production at the LHC

- NLO correction computed by Jones, Kerner and Luisoni (JKL) in 2018 using on-shell (OS) renormalization for the top quark (with $m_t^2 = 23m_H^2/12$).
- Two bugs found in 2021.

THEORY	LO [pb]	NLO [pb]
HEFT:	$\sigma_{\text{LO}} = 8.22^{+3.17}_{-2.15}$	$\sigma_{\text{NLO}} = 14.68^{+3.36}_{-2.64}$
FT _{approx} :	$\sigma_{\text{LO}} = 8.57^{+3.31}_{-2.24}$	$\sigma_{\text{NLO}} = 15.07^{+2.89}_{-2.54}$
Full:	$\sigma_{\text{LO}} = 8.57^{+3.31}_{-2.24}$	$\sigma_{\text{NLO}} = 16.01^{+1.99}_{-3.73}$

[Jones, Kerner and Luisoni 2018]

THEORY	LO [pb]	NLO [pb]
HEFT:	$\sigma_{\text{LO}} = 8.22^{+3.17}_{-2.15}$	$\sigma_{\text{NLO}} = 13.53^{+2.19}_{-2.04}$
FT _{approx} :	$\sigma_{\text{LO}} = 8.57^{+3.31}_{-2.24}$	$\sigma_{\text{NLO}} = 14.06^{+2.17}_{-2.25}$
Full:	$\sigma_{\text{LO}} = 8.57^{+3.31}_{-2.24}$	$\sigma_{\text{NLO}} = 14.19(7)^{+2.29}_{-2.23}$

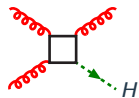
[Jones, Kerner and Luisoni 2021]

- Top quark only appears in virtual loops, so mass renormalization can give another hint (besides scale dependence) on the perturbative error.
- What about the bottom quark? In principle it can effect the p_T spectrum for low to intermediate p_T .

Goal: study Higgs + jet production with **exact top and bottom quark mass dependence**, assess dependence of results on the **choice of renormalization scheme**.

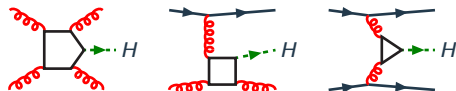
Higgs + jet production at the LHC: ingredients

Born



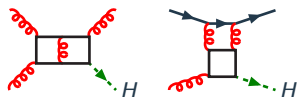
- Already one-loop at Born level
- Known since the late '80s [Ellis, Hinchliffe, Soldate and Van der Bij 1988]

Real



- Computed in the early 2000s [Del Duca, Kilgore, Oleari, Schmidh and Zeppenfeld 2001]
- Efficient implementation is key [Budge, Campbell, De Laurentis Ellis and Seth 2020]

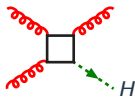
Virtual



- Top loop [Jones, Kerner and Luisoni 2018, Czakon, Harlander, Klappert and Niggetiedt 2021]
- Arbitrary quark masses [Bonciani, Del Duca, Frellesvig, Henn, Moriello and Smirnov 2016, all above + Hidding, Maestri and Salvatori 2019]

Higgs + jet production at the LHC: Born

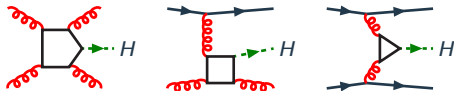
Born level amplitude is needed up to ϵ^2 (interference with virtual!)



- Sources of ϵ terms in the interference: polarizations of external particles (generate ϵ terms at interference level) and loop integrals (generate ϵ terms already at amplitude level).
 - Known analytically up to ϵ^0 : logs and Li_2 's.
- [Ellis, Hinchliffe, Soldate and Van der Bij 1988]
- Higher orders in the ϵ -expansion are computed using numerical methods, will be reviewed below.
 - For mass renormalization, also the derivative of the Born amplitude must be known (also obtained with numerical methods).

Higgs + jet production at the LHC: real radiation

Real radiation amplitude is needed up to ϵ^0



- First computed in the early 2000s

[Del Duca, Kilgore, Oleari, Schmidh and Zeppenfeld 2001]

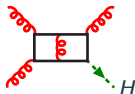
- These days, can be generated by loop matrix element providers: have generated the amplitudes with GoSam and MadGraph5_aMC@NLO.
- Perfect agreement is found including in single unsolved singular kinematic regions.
- Note that analytic formulae are much faster than loop providers: $\mathcal{O}(10^2)$
- Especially in light of a very efficient implementation based on methods exploiting unitarity cuts, implemented in MCFM-9.1 (used with a small hack to allow $\overline{\text{MS}}$ quark masses when needed).

[Budge, Campbell, De Laurentis Ellis and Seth 2020]

- Real radiation not the most time consuming part, even with loop providers.

Higgs + jet production at the LHC: virtual correction

Virtual correction: $gg \rightarrow gH$



$$\mathcal{M}_{gg \rightarrow gH} = f^{c_1 c_2 c_3} S_g^{\mu\nu\tau} \epsilon_{1,\mu}^{c_1} \epsilon_{2,\nu}^{c_2} \epsilon_{3,\tau}^{c_3}$$

$$S_g^{\mu\nu\tau} = \mathcal{F}_1 \mathcal{T}_{g,1}^{\mu\nu\tau} + \mathcal{F}_2 \mathcal{T}_{g,2}^{\mu\nu\tau} + \mathcal{F}_3 \mathcal{T}_{g,3}^{\mu\nu\tau} + \mathcal{F}_4 \mathcal{T}_{g,4}^{\mu\nu\tau}$$

- One color tensor structure only: $f^{c_1 c_2 c_3}$
- Form factor decomposition: 4 independent structures

$$\mathcal{T}_{g,1}^{\mu\nu\tau} = \frac{(s_{12} g^{\mu\nu} - 2p_2^\mu p_1^\nu)(s_{23} p_1^\tau - s_{13} p_2^\tau)}{2s_{13}}$$

$$\mathcal{T}_{g,2}^{\mu\nu\tau} = \frac{(s_{23} g^{\nu\tau} - 2p_3^\nu p_2^\tau)(s_{13} p_2^\mu - s_{12} p_3^\mu)}{2s_{12}}$$

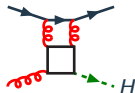
$$\mathcal{T}_{g,3}^{\mu\nu\tau} = \frac{(s_{13} g^{\mu\tau} - 2p_3^\mu p_1^\tau)(s_{12} p_3^\nu - s_{23} p_1^\nu)}{2s_{23}}$$

$$\mathcal{T}_{g,4}^{\mu\nu\tau} = \frac{1}{2} \left\{ g^{\mu\nu} (s_{23} p_1^\tau - s_{13} p_2^\tau) + g^{\nu\tau} (s_{13} p_2^\mu - s_{12} p_3^\mu) \right. \\ \left. + g^{\tau\mu} (s_{12} p_3^\nu - s_{23} p_1^\nu) + 2p_1^\nu p_2^\tau p_3^\mu - 2p_1^\tau p_2^\mu p_3^\nu \right\}$$

- Form factors \mathcal{F}_i are extracted using appropriate projectors: $\mathcal{P}_{g,i}^{\mu\nu\tau} S_{g,\mu\nu\tau} = \mathcal{F}_i$
- Number of Feynman diagrams: 288 (of which 18 involve one bottom quark)

Higgs + jet production at the LHC: virtual correction

Virtual correction: $q\bar{q} \rightarrow gH$



$$\mathcal{M}_{q\bar{q} \rightarrow gH} = t_{ij}^{c3} S_q^\tau \epsilon_{3,\tau}^{c3}$$

$$S_q^\tau = \mathcal{G}_1 \mathcal{T}_{q,1}^\tau + \mathcal{G}_2 \mathcal{T}_{q,2}^\tau$$

- One color tensor structure only: t_{ij}^{c3}
- Form factor decomposition: 2 independent structures

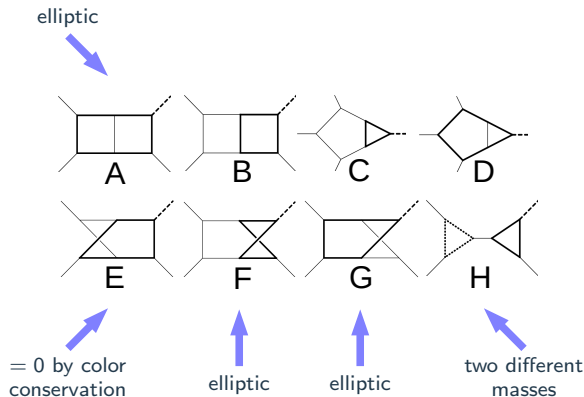
$$\mathcal{T}_{q,1}^\tau = p_1^\tau \not{p}_3 - \frac{1}{2} s_{13} \gamma^\tau,$$

$$\mathcal{T}_{q,2}^\tau = p_2^\tau \not{p}_3 - \frac{1}{2} s_{23} \gamma^\tau$$

- Form factors \mathcal{G}_i are extracted using appropriate projectors: $Tr(\mathcal{P}_i^\tau S_{q,\tau}) = \mathcal{G}_i$
- Number of Feynman diagrams: 51 (of which 2 involve one bottom quark)

Higgs + jet production at the LHC: 2-loop amplitude

The 2-loop amplitude is reduced to a set of master integrals (MIs) using standard tools



[(A,B,C,D): Bonciani, Del Duca, Frellesvig, Henn, Moriello and Smirnov 2016]

[(F): Bonciani, Del Duca, Frellesvig, Henn, Maestri, Moriello, Salvatori and Smirnov 2019]

[(G): Frellesvig, Hidding, Maestri, Moriello and Salvatori 2019]

Topologies

- Six 7-propagator integral families
- 4 scales: s , t , m_H , m_t

Reduction

- FIRE and Kira
- Total number of integrals: 479
- Of which 32 in H

Boundary conditions

- Computed at $s_{12} = s_{23} = m_H = 0$
- Most MIs vanish
- Rest reduce to known tadpoles and bubbles

Higgs + jet production at the LHC: 2-loop master integrals

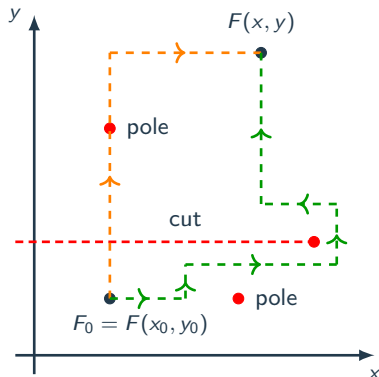
Values for the master integrals are obtained by a numerical solution of the differential equations: generalized power series solutions as implemented in the DiffExp package

[Moriello 2020, Hidding 2021]

- Identify a suitable path from the boundary condition to the physical point of interest.
- On each line segment, separately look for a solution of the form

$$F(s) = \sum_{j=0}^{\infty} \sum_{k=0}^N c_{j,k} (s-s_0)^{r+j} \ln^k(s-s_0), \quad r \in \mathbb{Q}$$

- Here s is a variable parametrizing the given line segment, while s_0 is a point on this segment where an initial condition is known.
- After substituting this form into the differential equation, determine the $c_{j,k}$'s algebraically.
- **Numerical accuracy can be increased** by retaining more terms in the ansatz.



Novel techniques are usually developed on general purpose platforms like Mathematica

- Very well suited to the exploratory phase of development.
- May not be appropriate for mass production of results.

A surprising bottleneck: software licenses

- CERN has 73 Wolfram Mathematica Kernel licenses and (73×8) 584 SubKernels
- Cannot really exploit the access to a CPU cluster with such numbers: not enough (Sub)Kernels for massive parallelization!

Important to bring these new techniques to lower level, open source environments!

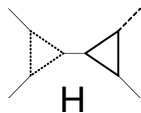
- Similar path of development with the NLO revolution

Aim: understand the impact of using different renormalization schemes for the internal quark and top-bottom interference

We renormalize the external fields on-shell and the strong coupling in a mixed scheme where running always depends on 5 light flavors.

Three setups differing in the radiative content and its treatment

1. **top(OS)**: the heavy quark contribution is renormalized at zero momentum, the Yukawa coupling and heavy quark mass in the on-shell (OS) scheme.
2. **top($\overline{\text{MS}}$)**: the Yukawa coupling and heavy quark mass are renormalized in the $\overline{\text{MS}}$ scheme.
3. **top+bottom($\overline{\text{MS}}$)**: the bottom quark is also included as a massive quark in all diagrams where it couples to the Higgs boson. For both the top and bottom quarks, the Yukawa couplings and heavy masses are renormalized in the $\overline{\text{MS}}$ scheme.
 - The “pure” QCD loop in topology H contains a massive top but massless bottom.
 - This allows the consistent use of 5-flavor PDF's and strong coupling.



Validating the 2-loop amplitudes

Several **technical checks** performed in order to validate the 2-loop amplitudes.

- **Infrared pole structure:** check that the infrared poles of the result agree with the known generic pole structure. ✓
- **EFT limit:** check convergence of the 1-loop and 2-loop full amplitudes to the tree-level and 1-loop result in the EFT as $m_q \rightarrow \infty$. ✓
- **IRC limits:** check that the behaviour of the matrix element in soft and collinear kinematic configurations agrees with the known universal formulae. ✓

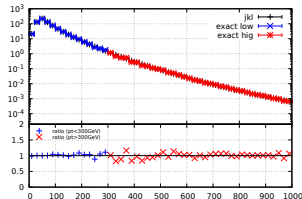
Tuned comparison to previous predictions: very good agreement with updated (2021) JKL [Jones, Kerner and Luisoni 2018] results for total cross section and Higgs boson p_T .

- This study

$$\sigma_{NLO} = 14.37 \pm 0.05 \text{ pb}$$

- JKL 2021 update

$$\sigma_{NLO} = 14.19 \pm 0.07 \text{ pb}$$



Setup

- pp collisions at $\sqrt{s} = 13$ TeV
- PDF set: NNPDF40_nlo_as_01180
- anti-kT jets with $R = 0.4$
- $p_T^i > 20$ GeV
- Scale variation: 7-point around $\frac{H_T}{2}$
- $m_H = 125.25$ GeV
- $m_t^{\text{OS}} = 172.5$ GeV
- $m_t^{\overline{\text{MS}}}(m_t^{\overline{\text{MS}}}) = 163.4$ GeV
- $m_b^{\overline{\text{MS}}}(m_b^{\overline{\text{MS}}}) = 4.18$ GeV
- $G_F = 1.16639 \cdot 10^{-5}$ GeV⁻²

$$\mu_R^0 = \mu_F^0 = \frac{H_T}{2} = \frac{1}{2} \left(\sqrt{m_H^2 + p_{\perp,H}^2} + \sum_i |p_{\perp,i}| \right)$$

Timing

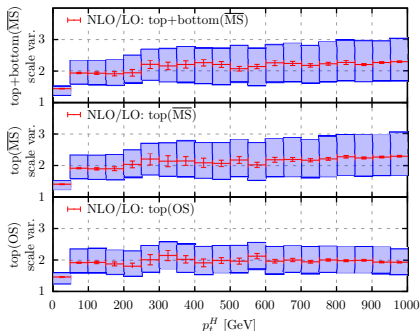
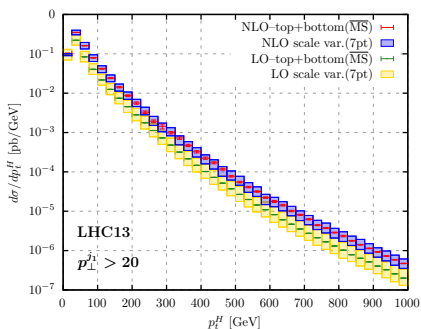
- Dominated by virtual.
- Generated a grid with $\mathcal{O}(100\text{k})$ points for the MIs: these pre-computed points serve as initial conditions for the numerical solution in phase space points (choose grid point “close to” the actual phase space point).
- Average runtime per phase space point depends strongly on the grid: from 5 min to 60 min with a median of around 15 min.

Integrated cross section

renormalisation of internal masses	σ_{LO} [pb]	σ_{NLO} [pb]
top+bottom-($\overline{\text{MS}}$)	$12.318^{+4.711}_{-3.117}$	$19.89(8)^{+2.84}_{-3.19}$
top-($\overline{\text{MS}}$)	$12.538^{+4.822}_{-3.183}$	$19.90(8)^{+2.66}_{-2.85}$
top-(OS)	$12.551^{+4.933}_{-3.244}$	$20.22(8)^{+3.06}_{-3.09}$

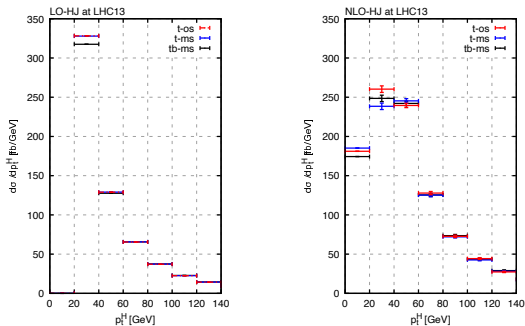
- From LO to NLO: large K -factor and reduction of scale uncertainties (from about 30% at LO to around 14% at NLO) in all three setups.
- Top-bottom interference is -0.2 pb at LO. The NLO correction is equal and opposite, cancelling the offset between the cross section with and without top-bottom interference.
- Dependence on top quark renormalization basically negligible at LO, at NLO the dependence is about 25 times bigger.

Higgs boson transverse momentum distribution



- Almost flat K -factor of 2 for top(OS), slightly larger for $\overline{\text{MS}}$ calculations.
- Smaller scale variation for top(OS) distribution, opposite to what is observed at the inclusive level.

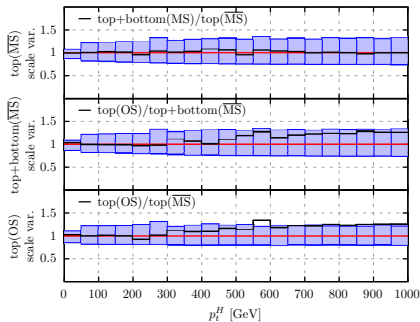
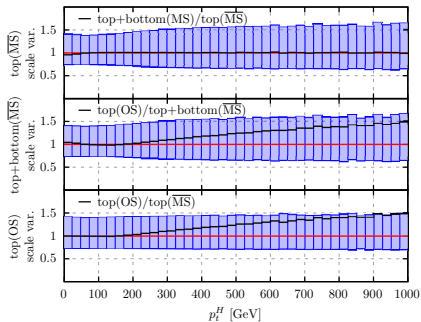
Higgs boson transverse momentum distribution at low p_T



- No events below 20 GeV at LO due to the kinematic cut on the jet.
- Observe the change of shape in this low p_T part of the spectrum.
- Increased sensitivity to renormalization scheme at NLO.
- Scale variation (not shown) much larger than the differences.

Higgs + jet production at the LHC: results

Ratios of differential distributions



- Going from LO (left) to NLO (right) we observe a reduction of scale uncertainty.
- But also the reduction of mass renormalization scheme dependence at large p_T .

Conclusions

Presented the rate for Higgs boson production in association with a hard jet at the LHC including NLO QCD corrections.

- NEW: full dependence on internal quark masses is retained.
- NEW: the top-bottom interference contribution is computed exactly (allowed by the excellent numerical stability)
- NEW: examined the impact of different mass renormalization schemes

Key takeaways

- Corrections to the interference term at NLO as large as the LO contribution and opposite in sign.
- Top-bottom interference effects change the shape of the Higgs transverse momentum distribution with respect to the computation with no interference.
- In the hard p_T tail, the top only calculation is fully justified, however the choice of mass renormalization scheme has an impact.

Building block for NNLO computation of Higgs production with arbitrary masses.

Possible to investigate top-charm interference as well.

This work was supported by grant K 143451 of the National Research, Development and Innovation Fund in Hungary and by the Bolyai Fellowship programme of the Hungarian Academy of Sciences.

Backup slides

Auxiliary mass flow (AMFlow): introduce an 'auxiliary mass' with every propagator

$$I = \int \prod_i \frac{d^d l_i}{(2\pi)^d} \frac{1}{D_1^{n_1} \cdots D_k^{n_k}} \quad \rightarrow \quad I^{\text{mod}}(\eta) = \int \prod_i \frac{d^d l_i}{(2\pi)^d} \frac{1}{(D_1 + i\eta)^{n_1} \cdots (D_k + i\eta)^{n_k}}$$

- The original integral is recovered as $I = \lim_{\eta \rightarrow 0} I^{\text{mod}}(\eta)$.
- Using IBP reduction, obtain a differential equation for the η -dependence of $I^{\text{mod}}(\eta)$

$$\frac{dI^{\text{mod}}(\eta)}{d\eta} = M(\eta)I^{\text{mod}}(\eta)$$

- Computation of the boundary condition (at $\eta \rightarrow \infty$) can be automated through an iteration of the procedure.
- Using this, a numerical solution can be constructed using generalized power series.

Compared the values of the full set of MIs in a number of physical phase space points to values obtained by the AMFlow package: always complete agreement with the full requested precision (16 digits).

Validating the 2-loop amplitudes: IR poles

Infrared pole structure is well known

$$\mathcal{M}_{gg,IR} = \mathbf{I}_{gg}(\{p\}, \epsilon) \sqrt{\alpha_s^3} \lambda \mathcal{M}_{gg,0} \quad \text{and} \quad \mathcal{M}_{q\bar{q},IR} = \mathbf{I}_{gg}(\{p\}, \epsilon) \sqrt{\alpha_s^3} \lambda \mathcal{M}_{q\bar{q},0}$$

with

$$\mathbf{I}_{gg}(\{p\}, \epsilon) = -\frac{\alpha_S}{\pi} (4\pi)^\epsilon e^{-\gamma\epsilon} \left(\frac{N_c}{\epsilon^2} + \frac{\beta_0}{\epsilon} \right) \left[\left(\frac{\mu^2}{-s} \right)^\epsilon + \left(\frac{\mu^2}{-t} \right)^\epsilon + \left(\frac{\mu^2}{-u} \right)^\epsilon \right]$$

$$\mathbf{I}_{q\bar{q}}(\{p\}, \epsilon) = -\frac{\alpha_S}{2\pi} (4\pi)^\epsilon e^{-\gamma\epsilon} \left\{ \frac{1}{N_c} \left[\frac{1}{\epsilon^2} + \frac{3}{2\epsilon} \right] \left(\frac{\mu^2}{-s} \right)^\epsilon - N_c \left[\frac{1}{\epsilon^2} + \frac{3}{4\epsilon} + \frac{\beta_0}{2N_c\epsilon} \right] \left[\left(\frac{\mu^2}{-t} \right)^\epsilon + \left(\frac{\mu^2}{-u} \right)^\epsilon \right] \right\}$$

```

# =====
# as= 0.11803734995855723
# v2= 60623.529110035874
# mh= 125.00000000000000
# mt= 173.05466381079322
# s= 4372281.0000000000
# t= -227168.49142857152
# u= -4129487.5085714282
# EFT gg: -9.000000000000000    35.878248503535914    -65.455554798888414    5.7566900428378968E-002
# EFT qa: -5.6666666666666670    18.647993884124027    -59.791910375745651    1.6681641403493153E-003
# EFT qq: -5.6666666666666670    28.505820966583826    -50.214695407176215    2.5460563703913090E-002
# EFT qq: -5.6666666666666670    18.838432322637775    -28.635770355000535    7.4227403480360446E-004
#
# FUL gg: -9.0000000000000018    35.878248503535900    -60.303874059251029    2.6235146505089173E-002
# FUL qa: -5.6666666666666679    18.647993884124016    -97.028566049524005    7.9201807450295471E-005
# FUL qq: -5.6666666666666670    28.505820966583833    -42.460365479670268    1.1157003297781931E-002
# FUL qq: -5.66666666666666581    18.838432322637725    12.655698706149482    2.1950637879329095E-005
# =====

```

$$\frac{2\pi}{\alpha_S \text{Born}} \cdot \left(\begin{array}{l} \text{double pole} \\ \text{single pole} \\ \text{finite part} \end{array} \right) \quad \text{Born at } \epsilon^0$$

Validating the 2-loop amplitudes: EFT limit

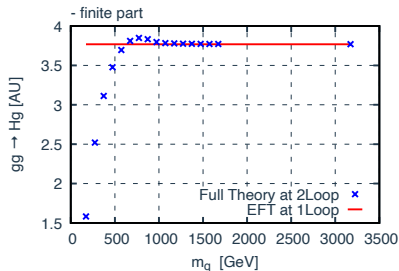
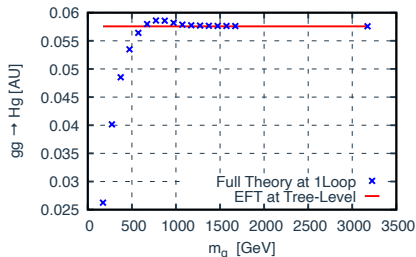
Effective field theory (EFT) limit: $m_q \rightarrow \infty$

- Expanding in the heavy quark mass,

$$V_2 = c_0 + \frac{c_1}{m_q^2} + \frac{c_2}{m_q^4} + \dots$$


the EFT limit checks c_0 .

- Note the nice convergence of the 1-loop and 2-loop full amplitudes to the tree-level and 1-loop result in the EFT.
- The rest of the series with dimensionful coefficients is however divergent in the collinear and soft limit.



The behaviour of matrix elements in soft and collinear limits is universal and well-known.

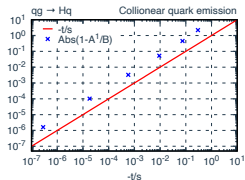
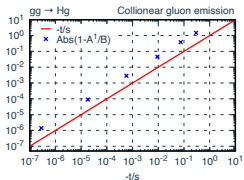
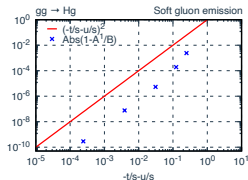
- Used the well-known factorization formulae to build CoLoRFuNNLO counterterms to the 1- and 2-loop $H + j$ matrix elements [Catani and Grazzini 2000, Bern, Del Duca, Kilgore and Schmidh 1999, Kosower 1999, Bern, Del Duca and Schmidh 1998, Bern, Dixon, Dumbbar and Kosower 1994]
- The counterterms reproduce the divergent soft and collinear limits of the 2-loop matrix element in terms of universal soft and collinear splitting functions and lower-point and lower-loop matrix elements.

<p>soft</p> $\langle a \mathcal{M}^{(1)}(q, p_1, \dots, p_m) \rangle \simeq g_S \mu^\epsilon \epsilon^\mu(q) \left[J_\mu^{a(0)}(q) \mathcal{M}^{(1)}(p_1, \dots, p_n) \rangle + g_S^2 \mu^{2\epsilon} J_\mu^{a(1)}(q, \epsilon) \mathcal{M}^{(0)}(p_1, \dots, p_n) \rangle \right]$	<p>collinear</p> 
--	---

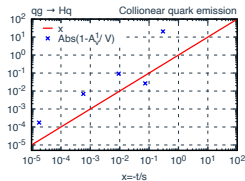
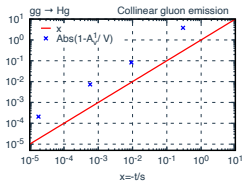
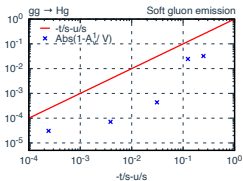
- Exact 2-loop $gg \rightarrow H$ matrix elements used to build counterterms [Aglietti, Bonciani, Degrassi and Vicini 2006, Anastasiou, Deuschmann and Schweitzer 2020]
- Checked that the full $H + j$ amplitude (1- and 2-loop) reproduce the expected singular behaviour.
- This exercise was done also for individual pieces, e.g., the 2-loop photon correction that probes the planar part or the OS mass and Yukawa renormalization pieces.

Validating the 2-loop amplitudes: IRC limits

One-loop squared matrix elements



Two-loop squared matrix elements



- Behaviour similar for internal quark masses from $\mathcal{O}(1 \text{ GeV})$ to physical top mass.
- Also with one large and one small internal mass ($y_t y_b$ term $>$ cancellation)

Validating the 2-loop amplitudes: checks against previous results

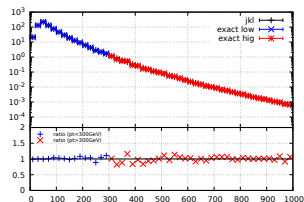
Tuned comparison to JKL [Jones, Kerner and Luisoni 2018]: very good agreement with their updated (2021) results for total cross section and Higgs boson p_T .

- This study

$$\sigma_{NLO} = 14.37 \pm 0.05 \text{ pb}$$

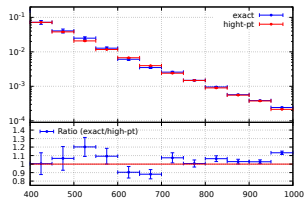
- JKL 2021 update

$$\sigma_{NLO} = 14.19 \pm 0.07 \text{ pb}$$



The hard tail of the distribution is compared to the prediction based on the computation of the relevant amplitudes in the high p_T range [Melnikov, Kudashkin and Wever 2018, Lindert, Melnikov, Kudashkin and Wever 2018].

- Tuned comparison of the implementation of this process in MCFM-9.1 with the exact result.



The 2-loop amplitude framework

Two-loop amplitudes implemented through a MadGraph5_aMC@NLO plugin were

$$\mathcal{M}_{gg \rightarrow gH} = f^{c_1 c_2 c_3} \mathcal{S}_g^{\mu\nu\tau} \epsilon_{1,\mu}^{c_1} \epsilon_{2,\nu}^{c_2} \epsilon_{3,\tau}^{c_3} \quad \text{and} \quad \mathcal{M}_{q\bar{q} \rightarrow gH} = t_{ij}^{c_3} \mathcal{S}_q^{\tau} \epsilon_{3,\tau}^{c_3}$$

appear as effective vertices in a UFO model.

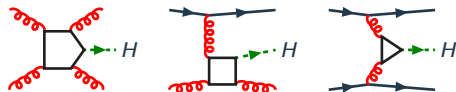
- Form factors are evaluated via a Mathematica interface that uses the DiffExp package to compute the MIs for each phase space point and inserts the results into the relevant formulae.
- Form factors are then inserted into a tree-level matrix element code (Fortran).

This approach greatly facilitates distribution and reproducibility of the 2-loop amplitude and offers flexibility in selecting the contributions the user is interested in, e.g.,

- choice of OS vs. $\overline{\text{MS}}$ renormalization scheme
- selecting particular interference terms and quark flavors in each loop
- renormalization scale variation through reweighting: compute form factors only once
- potential to attach Higgs boson decay to the production process

Note that by interfering full amplitudes, when we include the contribution of the bottom quark, we are in fact computing $Ay_t^2 + By_t y_b + Cy_b^2$, i.e., all three contributions.

Infrared and collinear (IRC) singularities in real radiation treated using subtraction



- Used Catani-Seymour dipole subtraction as implemented in MCFM-9.1.
- Cross-checked with an implementation of CoLoRFulNNLO subtraction as well as with an implementation of NLO dual dipoles.

[GS 2009, Prisco and Tramontano 2021]

- Implementation strategy: for simplicity, defined integrated subtractions in terms of the Born matrix element only up to ϵ^0 . Pole cancellation then requires a rearrangement of the coefficients of the Laurent expansion of the interference among the 1-loop and 2-loop diagrams.